JOURNAL OF MATERIALS SCIENCE **34** (1999) 4209–4218

Fracture behaviour of accelerated aged solid rocket propellants

KYM M. IDE, SOOK-YING HO
Weapons Systems Division, Defence Science and Technology Organisation, Salisbury SA 5108, Australia

DAVID R. G. WILLIAMS
Department of Chemical Engineering, University of Adelaide

The effect of temperature, strain-rate and ageing on the crack growth mechanism in a composite propellant has been examined to obtain an understanding of the fracture process under service life conditions. Both as-received and aged specimens were tested at each of three strain-rates and temperatures. The materials were aged by subjecting them to various thermal loads (accelerated ageing, thermal cycle and thermal shock) designed to expose them to conditions similar to that experienced by a rocket motor during its service life. The fracture behaviour of the propellant specimens were affected by changes in temperature whilst strain-rate had only a marginal effect over the range studied. It was found that as the material temperature decreased from 60 to $-40\,^{\circ}$C the stiffening of the propellant caused increased hysteresis ratios and decreased crack velocities. The deterioration of the mechanical properties of the propellant depended on the severity of the thermal loads. In each case the accelerated aged specimens became harder and more brittle whilst the thermally cycled and thermally shocked specimens were only marginally affected. A distinct difference in the mechanism of crack growth was observed for the accelerated aged specimens, along with a marked decrease in hysteresis ratio, critical stress and critical strain and an increase in crack velocity.

1. Introduction

An understanding of the fracture behaviour of solid composite propellants is important in service life analysis of rocket motors. A crack propagating in a propellant grain creates extra surface area for burning which affects the ballistic performance of the rocket motor. Significant insight into the mechanism of crack extension in a filled polymer has been achieved by the use of acoustic imaging, X-ray imaging, photographic and video records. Liu [1–4] determined that a clearly defined near tip mechanism exists and that the effects of temperature and strain-rate only alter this mechanism in a quantitative (but not qualitative) manner.

Liu [1] employed high energy real-time X-ray imaging to examine the local fracture processes near the crack tip in an inert solid propellant. Microcracks generated ahead of the crack tip in a damage or failure zone increase in number with the applied strain. Crack extension results from the coalescence of large microcracks with the main crack tip. The crack growth was described as proceeding in a zigzag direction via a mechanism that included crack-tip blunting and resharpening.

In a study of edge cracked biaxial stressed solid propellant specimens Smith and Liu [2] described the crack growth as a highly non-linear process. During a period of crack tip blunting voids formed in the damage zone ahead of the crack, this was followed by a period of crack resharpening and growth. It was found that in a global sense the crack grew in a plane normal to the direction of specimen extension. However, the crack path was locally undulating with growth accomplished by the crack tip connecting with voids ahead of it. A clear difference between low temperature and above zero testing was observed. The low temperature tests suggested a much stiffer response, with much greater values of initial modulus and maximum load. An absence of crack blunting at the low temperature was noted and ascribed to binder stiffening producing a transverse constraint at the crack tip which caused the material to behave as a single phase continuum.

The degradation of a propellant's mechanical properties when subjected to thermal loads increases the likelihood of material cracking or bondline failure occurring. Liu [3] investigated the consequences of "pre-damage" on crack growth behaviour in thin sheet specimens of propellant by stretching to 15% strain and then unloading. An acoustic imaging system was employed to examine the crack growth on re-straining. When pre-damaged and virgin specimens with and without cracks were compared Liu found that larger damage zones with higher damage intensities were seen ahead of crack tips in pre-damaged specimens. Therefore, pre-damage in a specimen may induce different material response and crack growth behaviour as compared to a virgin

specimen. In a similar study Liu [4] found that the crack velocity in an undamaged highly filled polymeric material was significantly lower than that for pre-damaged specimens.

This paper reports on a detailed examination of the effect of temperature, strain-rate and ageing on the crack growth mechanism in a composite propellant to obtain an understanding of the fracture process under service life conditions.

2. Experimental

In this study, the crack growth behaviour in a highly filled composite propellant was investigated. Specimens of propellant were prepared from hydroxy-terminated polybutadiene (R45-M) and two size ranges ("coarse" and "fine") of ammonium perchlorate (AP). The propellant mix was cast into rectangular teflon lined molds and held at 60 °C for a total of 216 h during cure.

To investigate the crack growth behaviour of aged propellant a quantity of the cured slabs were placed in thermal conditioning chambers and aged according to three thermal loads (see Table I) which simulate the ageing environments commonly encountered by in-service rocket motors.

Specimens of dimension $125 \times 40 \times 10$ mm were milled from aged and unaged slabs and a 10 mm razor blade cut inserted at the edge of the specimen to form the initial sharp crack. The specimens were bonded to mild steel grips with a thin layer of epoxy resin prior to loading into the Instron tensile testing machine. The specimen geometry was chosen so that the 125 mm length would provide a sufficiently long distance to follow the propagating crack and allow ample data to be recorded for calculating the crack velocity.

Prior to conducting the fracture tests, hysteresis losses for aged and unaged specimens of propellant at three temperatures (−40, 25 and 60 °C) at each of three crosshead speeds (0.2, 0.5 and 1.0 $cm \cdot min^{-1}$) were measured. Specimen geometry and loading condition was the same as that described for the crack propagation study, except that no initial crack was present.

Each fracture test consisted of extending the specimen at constant crosshead speed in the Instron tensile testing machine until failure. The applied load was recorded by a computer linked to the Instron load cell via an analogue to digital converter. Specimens of unaged propellant and those subjected to each of the thermal loads were tested at temperatures of −40, 25 and 60 °C at each of three crosshead speeds (0.2, 0.5 and 1.0 $cm \cdot min^{-1}$).

The progress of the crack as it propagated through the specimen was followed by a travelling microscope with a S-VHS camera/recorded attached. The distance the travelling microscope moved was measured by a micrometer fixed into the mount. The highly magnified image captured the crack opening in detail and allowed precise identification of the onset of crack propagation. A digital frame numbering device allowed accurate identification of the time between events on the videotape record and a LED triggered at the test start was placed in the field of view of the microscope. A graticule which was internally fitted into the microscope enabled the calculation of the increase in crack length. Images of the propagation of cracks in aged and unaged specimens recorded to videotape have been captured and magnified to highlight the area of interest, the original colour videotape is reproduced in the figures as 256 levels of grey.

TABLE I Thermal loads for propellant ageing

	Accelerated ageing	Thermal shock	Thermal cycle
Step 1	64 °C for 16 weeks	60 °C for 16 h	45 °C for 30 days
Step 2	Equilibrate at 25 °C	Equilibrate at 25 °C	Equilibrate at 25 °C
Step 3		−40 °C for 8 h	−30 °C for 20 days
Step 4		Equilibrate at 25 °C	Equilibrate at 25 °C
Steps repeated	×1	×10	×5

3. Results and discussion

3.1. Dependence of crack growth behaviour on temperature

The image shown in Fig. 1 corresponds to a time immediately after the application of the load to an unaged propellant specimen. The initial razor blade cut can be seen between graticule marks 50 and 66, the crack has not yet begun to propagate. A concentrated zone of damage (marked on the image) has formed ahead of the crack, whilst the tip itself remains blunt, it consists of elongated fibrils of HTPB binder and dewetted filler particles.

The AP particles in the damage zone dewet soon after the application of the stress causing the formation of small voids around the filler particles and fibrils of HTPB binder. As the strain increases the voids coalesce and the fibrils rupture at thinned sections of material strained between filler particles or debond at the binder/filler interface. The crack propagates into the damage zone by coalescing with the voids and microcracks as the fibrils fail. Evidence from Scanning Electron Microscopy (SEM) [5] indicates that the particles of AP do not fracture, rather the crack propagates around them via breakage of the fibrils. The crack was observed to extend perpendicular to the direction of the applied load but locally it deviated above and below the particles of AP in a random manner, which was also evident from the jagged appearance of the fracture surface.

The shape of the crack tip as it propagates into the specimen can be described as a cycle of blunt-sharp-blunt. Fig. 2 shows the resharpened shape of the crack tip after it had propagated approximately the length of the damage zone. The crack then blunts as a new damage zone forms in the area ahead of the crack tip at graticule mark 41.

A SEM of the fracture surface of the unaged specimen of propellant is shown in Fig. 3. Circular holes can be seen where dewetted AP particles were dislodged and remained in the other fracture surface. As expected

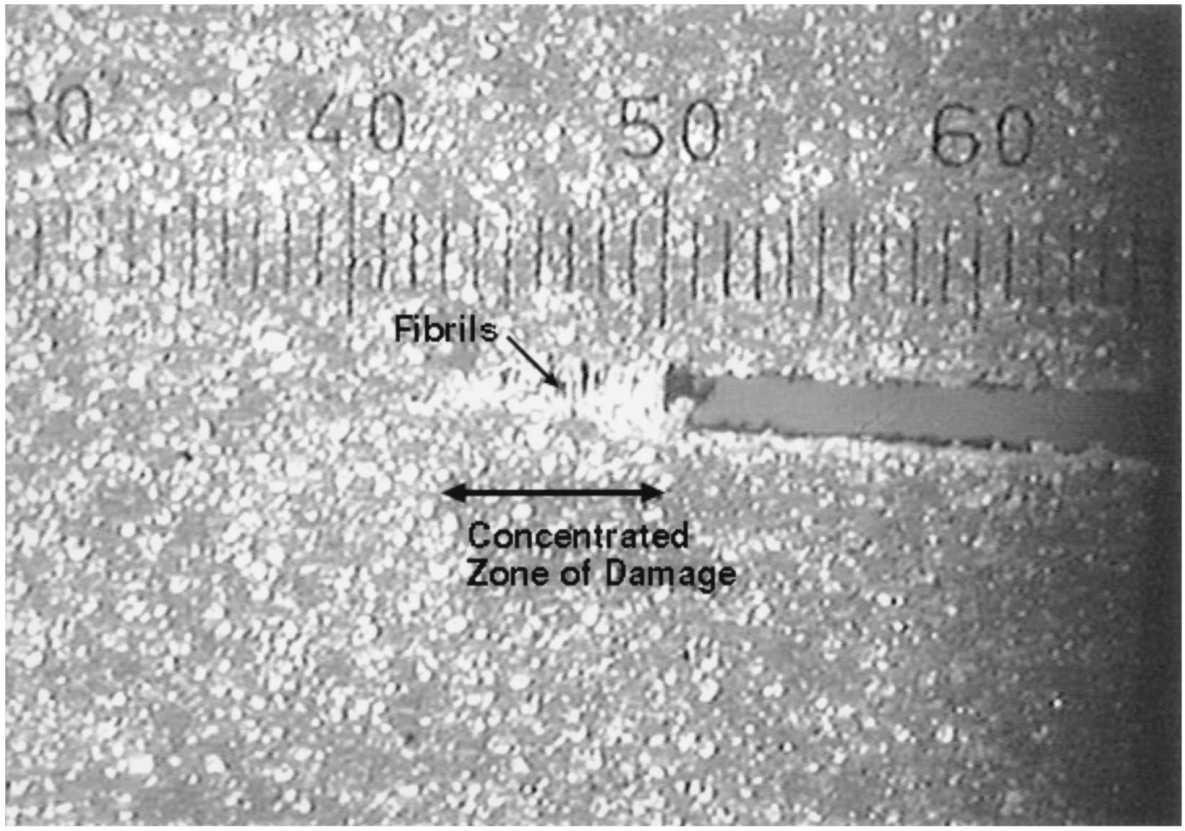

Figure 1 Propellant unaged, $T = 25\,^{\circ}\mathrm{C}$, $\varepsilon = 4.1\%$.

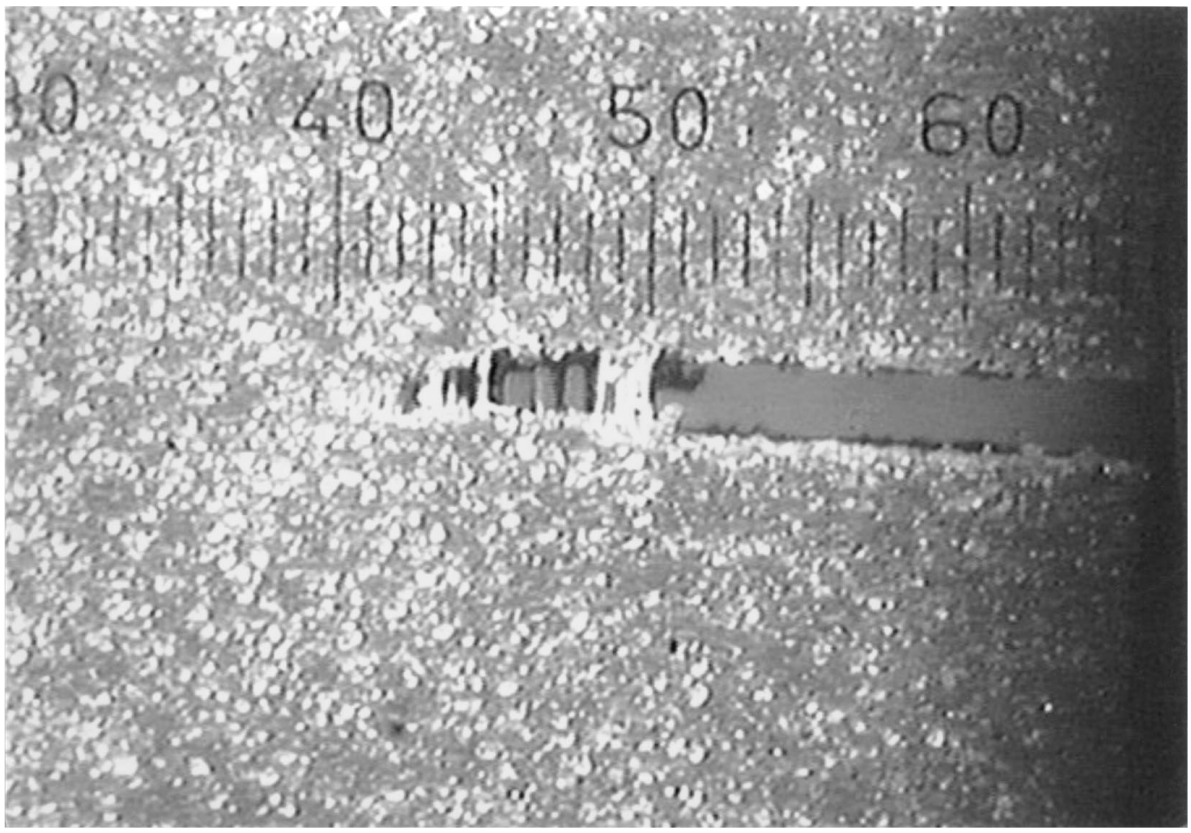

Figure 2 Propellant unaged, $T = 25\,^{\circ}\mathrm{C}$, $\varepsilon = 4.5\%$.

the AP particles were not fractured rather the crack deviated over or under the individual particles.

The damage zone and crack propagation response for an unaged propellant specimen tested at 60 °C is presented in Figs 4 and 5. The fibrils present at 3.3% strain have failed at 3.6% and the crack tip is in a state of temporary arrest while the damage zone increases in size. The mechanism of crack growth was the same as that

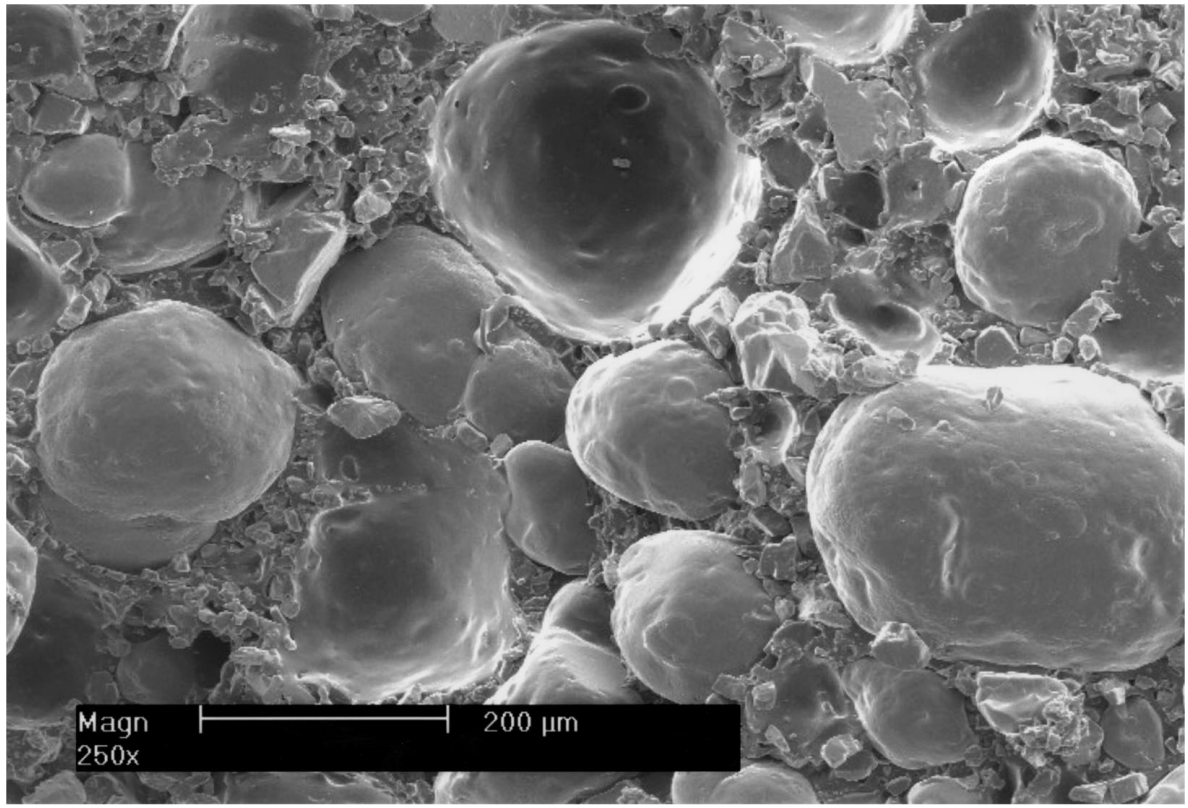

Figure 3 SEM showing centre of fracture surface in unaged propellant, $T = 25\,^{\circ}\mathrm{C}$.

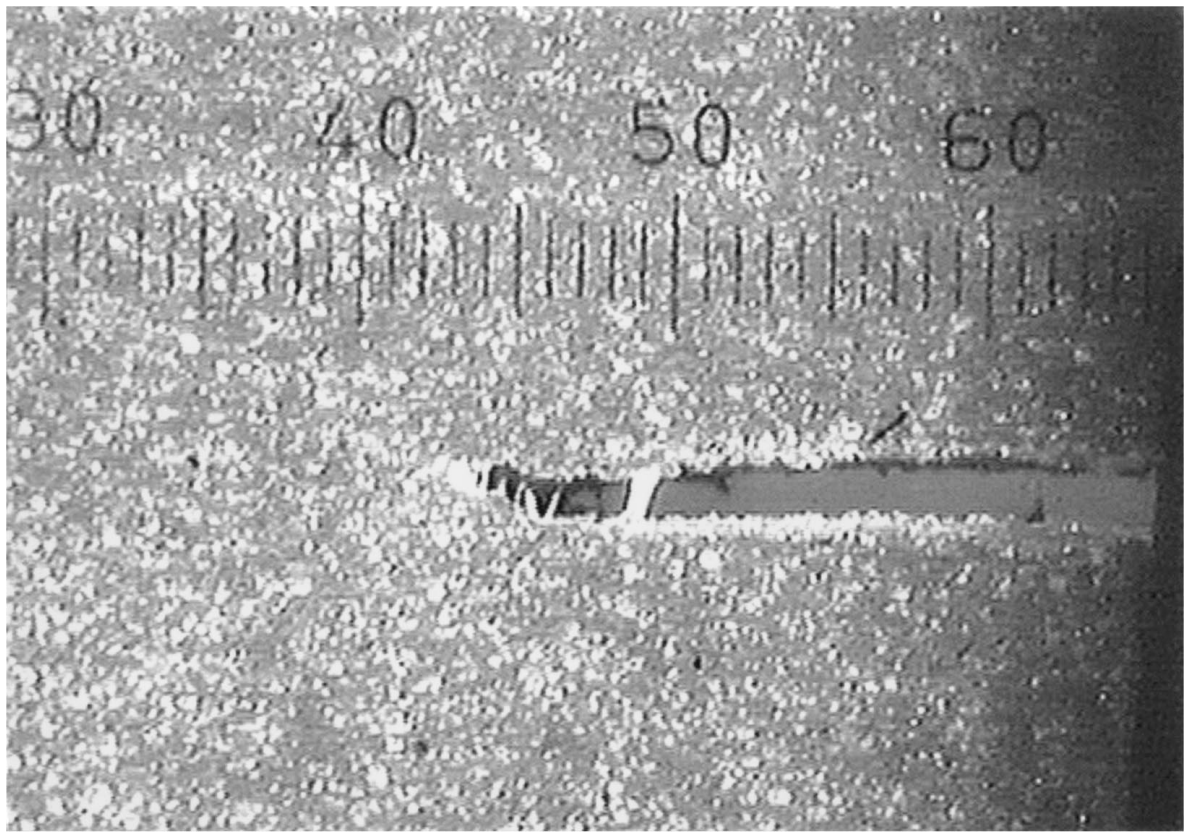

Figure 4 Propellant unaged, $T = 60\,^{\circ}\mathrm{C}$, $\varepsilon = 3.3\%$.

seen in the tests at 25 °C, however, the size of the damage zone and the level of strain at crack propagation was lower, this was reflected in higher crack velocities (see later discussion). In the unaged propellant at 25 °C immediately prior to crack propagation the damage zone measured approximately 4.5 mm in length and 1.3 mm in height. In the unaged propellant at 60 °C the area of damage that could be clearly distinguished was 2.8 mm in length and the fibrils at the crack tip were 0.83 mm in height. The similarity in the crack growth mechanism

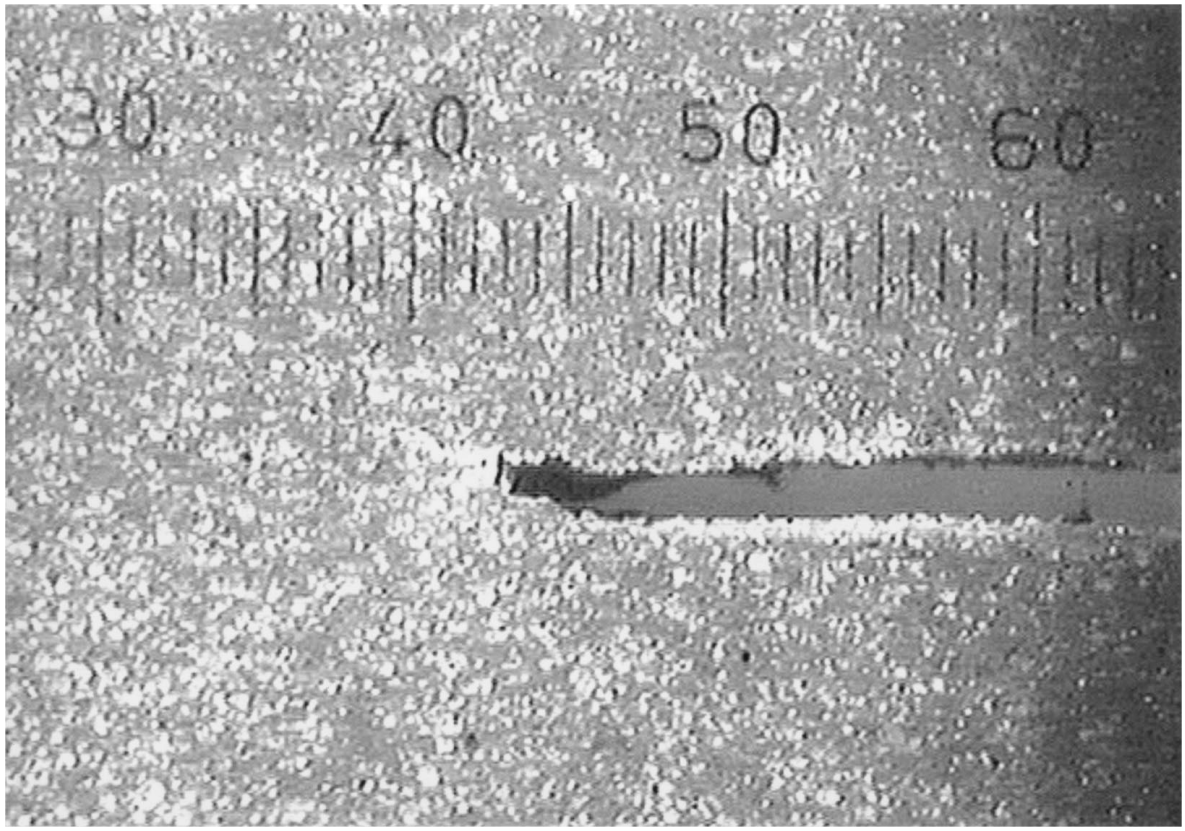

Figure 5 Propellant unaged, $T = 60\,^{\circ}\mathrm{C}$, $\varepsilon = 3.6\%$.

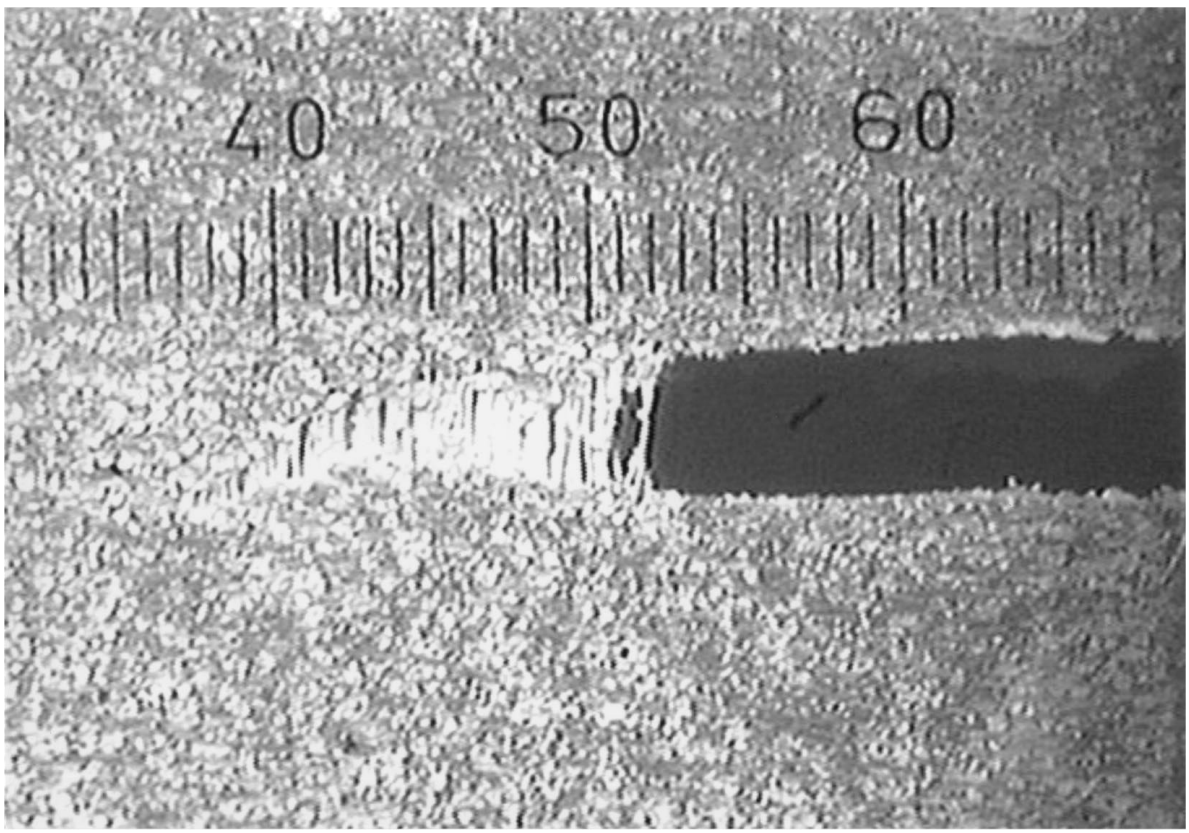

Figure 6 Propellant unaged, $T = -40\,^{\circ}\mathrm{C}$, $\varepsilon = 6.0\%$.

at ambient (22 °C) and elevated (74 °C) temperatures was also described in the study by Smith, *et al.* [6].

Unaged propellant tested at −40 °C is shown in Fig. 6. The crack was observed to propagate by the mechanism outlined above. The initial damage zone prior to crack propagation attained a maximum length of 18.3 mm and the fibrils at the crack tip were 5.3 mm in height, an area substantially greater than those at

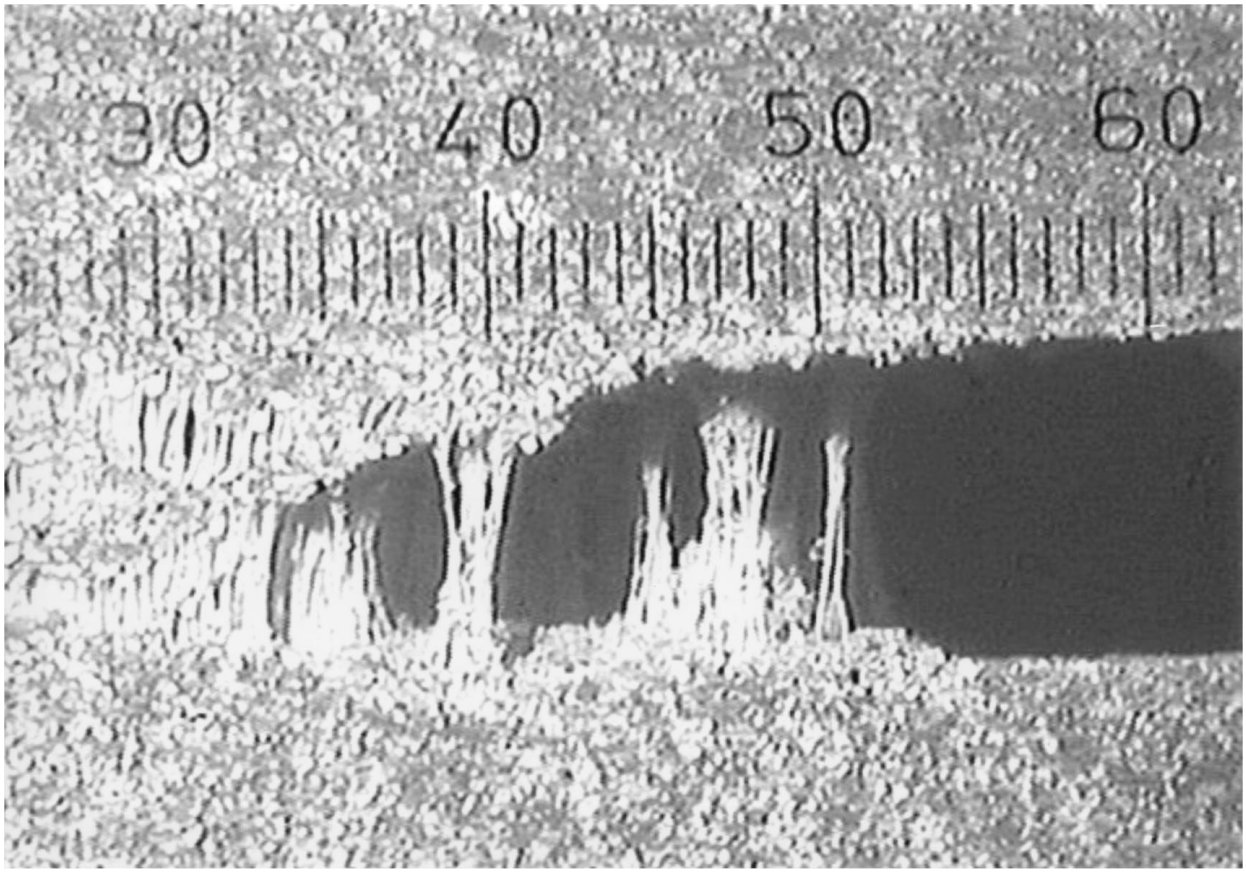

Figure 7 Propellant unaged, $T = -40\,^{\circ}\mathrm{C}$, $\varepsilon = 10.5\%$.

TABLE II Values of hysteresis ratio[a], h_r, for $\dot{\varepsilon} = 0.0037\ s^{-1}$

T(°C)	Unaged	Thermal shock	Thermal cycle	Accelerated ageing
−40	0.41	0.41	0.40	0.35
25	0.39	0.37	0.36	0.32
60	0.32	0.29	0.28	0.26

[a] $h_r = H/W_i$, where H is the hysteresis strain energy density and W_i, the input strain energy density.

temperatures above zero. The higher hysteresis ratio measured at −40 °C compared to those measured above 0 °C (see later section and Table II), reflects the greater energy losses.

In Fig. 7 the crack has advanced only a fraction of the length of the damage zone. At this point it was observed that multiple damage zones were forming throughout the specimen. The loss processes in these zones contribute to the overall irreversible energy losses and were widely distributed over the specimen. As the strain increased these secondary cracks began to propagate eventually connecting with the original crack and leading ultimately to specimen failure.

The measured hysteresis ratio (energy losses), due to dissipation mechanisms such as dewetting, microvoiding and microcracking [7] are listed in Table II. The larger damage zones observed at −40 °C, compared to those at 25 and 60 °C, are consistent with the higher values of hysteresis ratio measured at the lower temperatures, (hysteresis ratio decreased from 0.41 to 0.32 when the temperature changed from −40 to 60 °C) for the unaged propellant.

3.2. Dependence of crack growth behaviour on strain-rate

Crack propagation and hysteresis tests were carried out at each of the three strain-rates detailed in the experimental method. The increase in the hysteresis ratio with strain-rate for specimens subjected to the same thermal loading is shown in Fig. 8. An increase in the crack velocity and decrease in the strain level required for crack propagation was also measured as the strain-rate increases, see Fig. 12. There was a marginal increase in the size of the damage zones with strain-rate.

3.3. Dependence of crack growth behaviour on thermal load

The crack propagation in a specimen of propellant that had been subjected to accelerated ageing conditions is shown in Fig. 9. On application of the load the crack propagated very quickly across the specimen. The shape of the crack was sharp at all times with no evidence of blunting. A similar crack growth mechanism was observed in accelerated aged propellant at 60 °C, however, the critical stress decreased. The ageing process has resulted in the binder becoming brittle and hardened with a subsequent reduction in the strain to failure of the propellant. The crack propagated at a strain of 1% as compared to 4% for the unaged material (at 25 °C and $0.0037\ s^{-1}$).

A SEM photograph (Fig. 10) shows the fracture surface of a propellant specimen which had been accelerated aged. A significant difference to the unaged material was the appearance of fractured particles in the

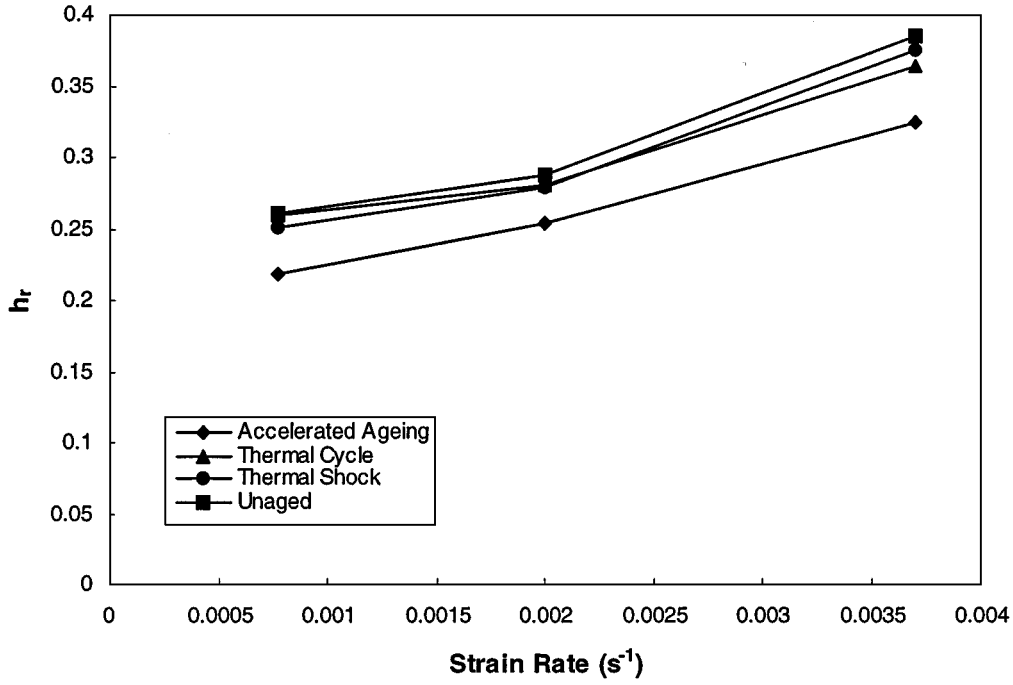

Figure 8 Change in hysteresis ratio with strain-rate for propellant ($T = 25\,^{\circ}$C).

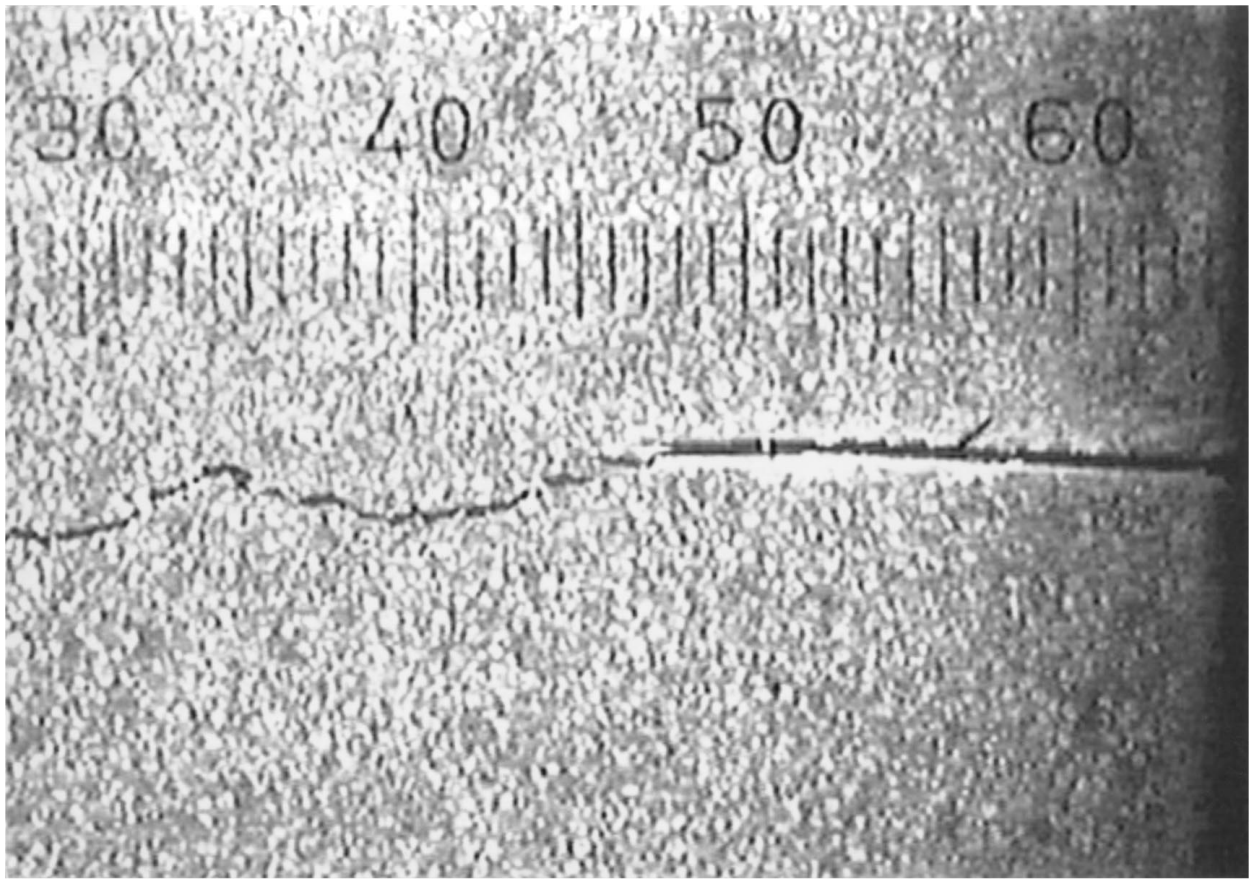

Figure 9 Propellant accelerated aged, $T = 25\,^{\circ}$C, $\varepsilon = 1.5\%$.

surface (as outlined on the image). The crack growth mechanism appears to include some particle fracture. When subjected to accelerated ageing the AP particles decompose and the propellant becomes more brittle [8]. A damage zone was not detected on the videotape record of the crack propagation therefore the large energy losses associated with more extensive dewetting and fibril formation were absent. This was confirmed by the measured values of hysteresis ratio for the accelerated aged propellant which was significantly lower than that of the other propellant specimens at each temperature (see Table II and Fig. 12).

Fig. 11 shows the crack growth at $-40\,^{\circ}$C in an accelerated aged specimen of propellant. The crack has

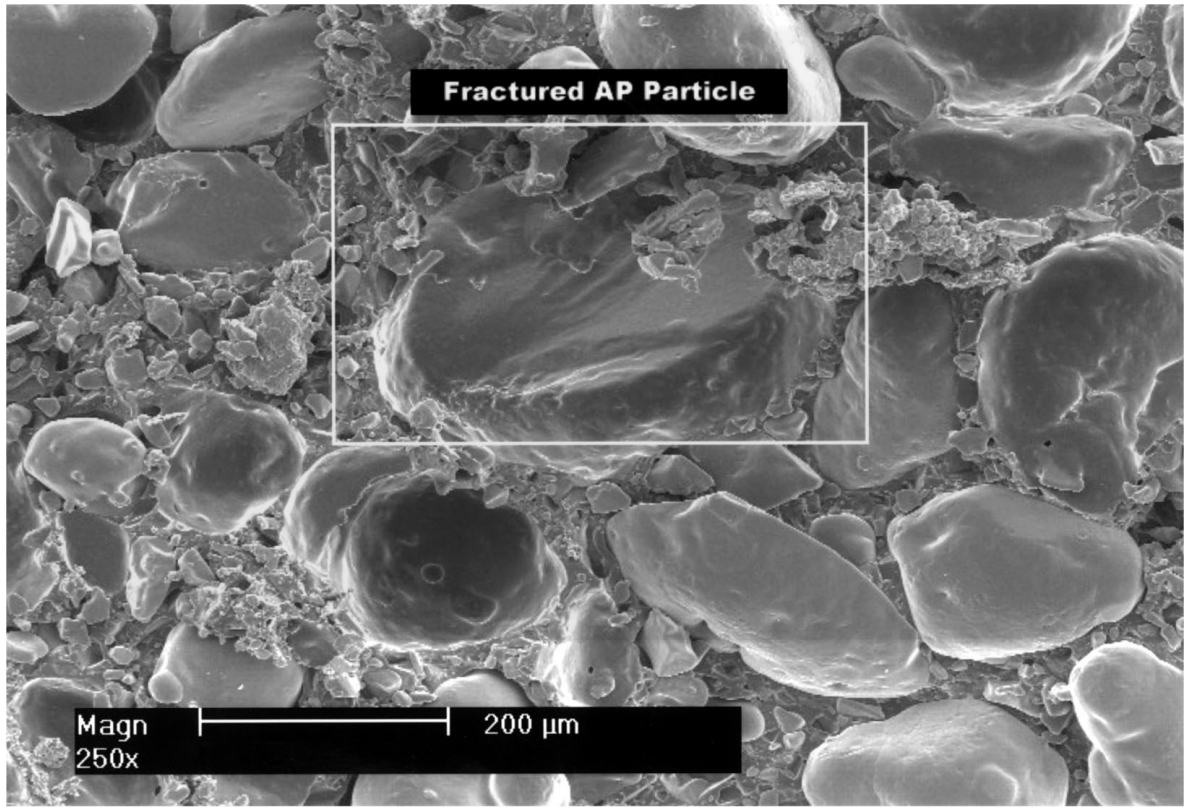

Figure 10 SEM showing fracture surface in accelerated aged propellant, $T = 25\,^{\circ}\mathrm{C}$.

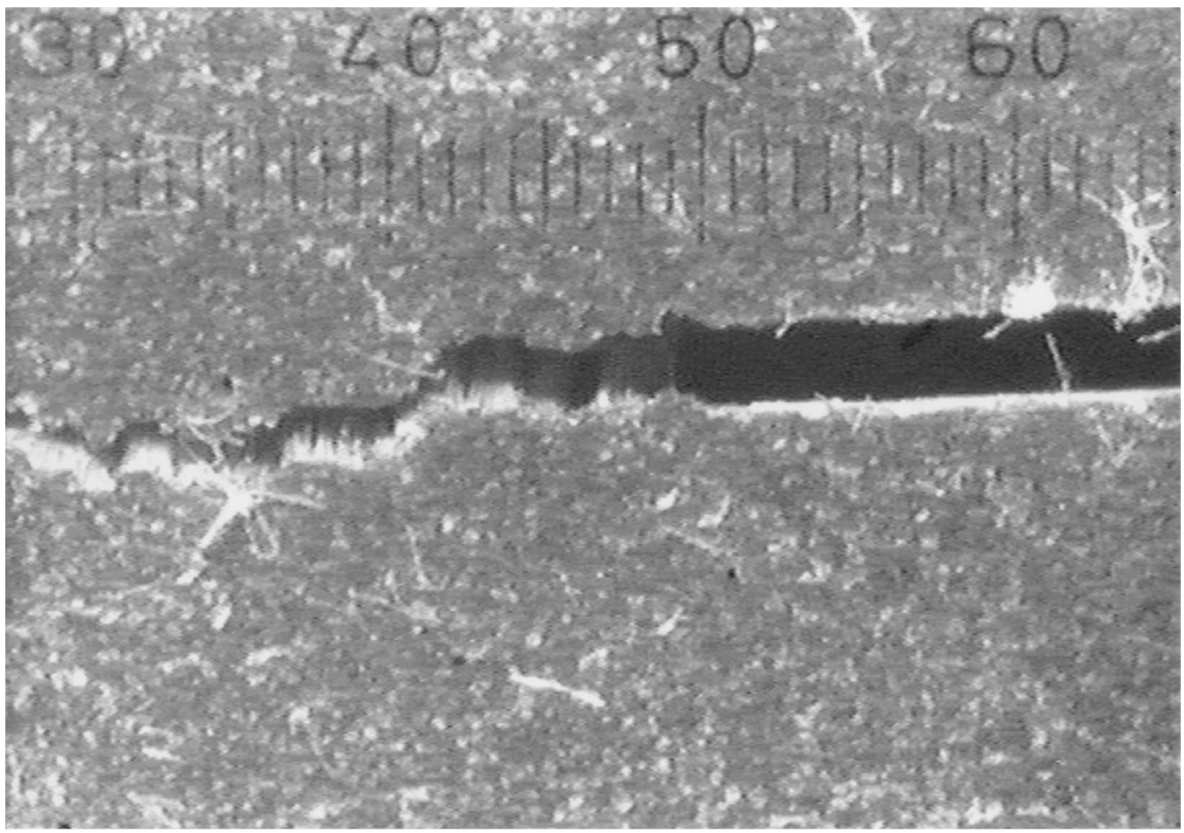

Figure 11 Propellant accelerated aged, $T = -40\,^{\circ}\mathrm{C}$, $\varepsilon = 3.7\%$.

propagated rapidly without the formation of a damage zone along the length of the specimen, however, a small number of fibrils formed in the centre of the specimen did not fail immediately. As increase in hysteresis ratio was observed at $-40\,^{\circ}\mathrm{C}$.

The mechanism of crack growth in specimens of propellant which had been subjected to thermal shock and thermal cycle loadings was observed to be the same as that in the unaged propellant and the size of the damage zones were similar in magnitude. Similar levels of

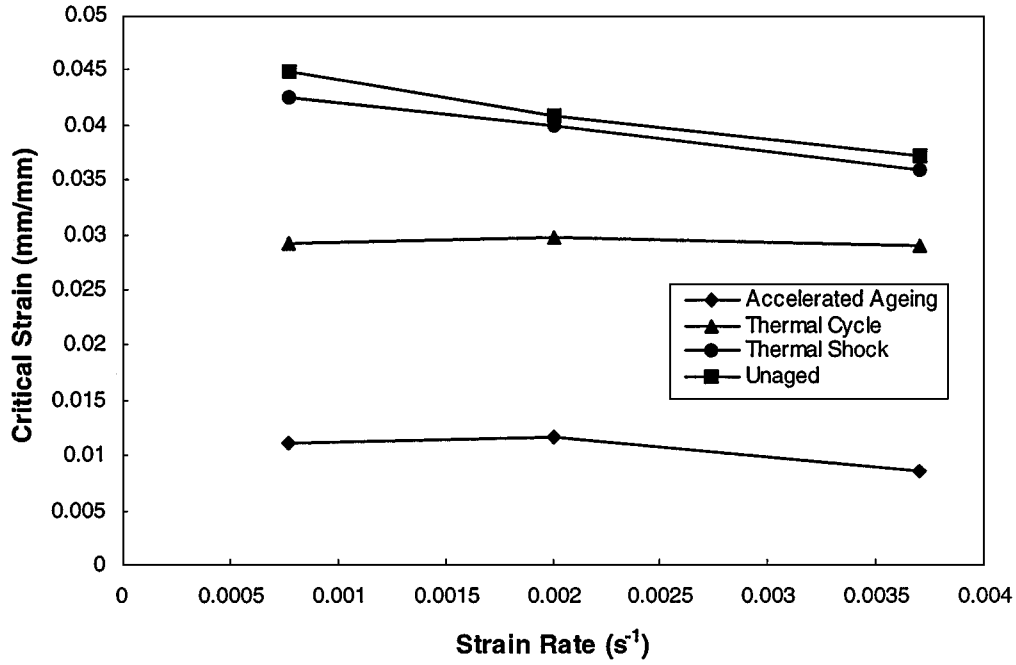

Figure 12 Change in critical strain with strain-rate for propellant ($T = 25\,^{\circ}$C).

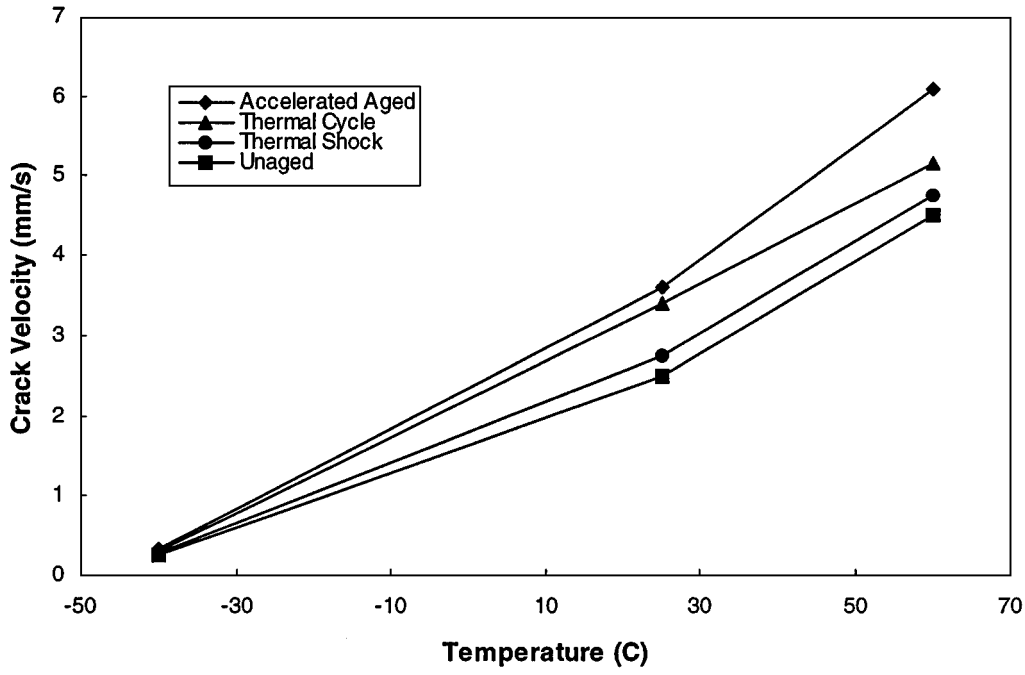

Figure 13 Crack velocity in propellant specimens ($\dot{\varepsilon} = 0.002\ \mathrm{s}^{-1}$).

hysteresis energy losses were measured, see Table II. However, the critical stress was greater and the critical strain lower than those measured for the unaged propellant (see Fig. 12).

The average crack velocity for propellant specimens subjected to various ageing conditions is plotted in Fig. 13. The specimens subjected to thermal shock had crack velocities slightly greater than that measured in the unaged propellant ($4.75\ \mathrm{mm \cdot s^{-1}}$ as compared to $4.50\ \mathrm{mm \cdot s^{-1}} \pm 0.02\ \mathrm{mm \cdot s^{-1}}$ at $60\,^{\circ}$C). The crack velocities increased further for the thermally cycled specimens to $5.17\ \mathrm{mm \cdot s^{-1}}$. For the accelerated aged specimens, no damage zone was observed during the crack propagation tests and the resulting crack velocity was the maximum for the specimens tested, $6.10\ \mathrm{mm \cdot s^{-1}}$.

A correlation exists between the size of the damage zone, specimen temperature and crack velocity. As the severity of the thermal load to which the propellant specimen had been subjected or as specimen temperature decreased, higher levels of crack blunting and larger damage zones resulted. The magnitude of the crack velocity was directly affected by the level of impedance to crack propagation caused by blunting. Another contributing factor is the decrease in activation energy barrier for crack propagation with increasing temperature, which follows from the kinetic approach to fracture [9]. As the material temperature increases

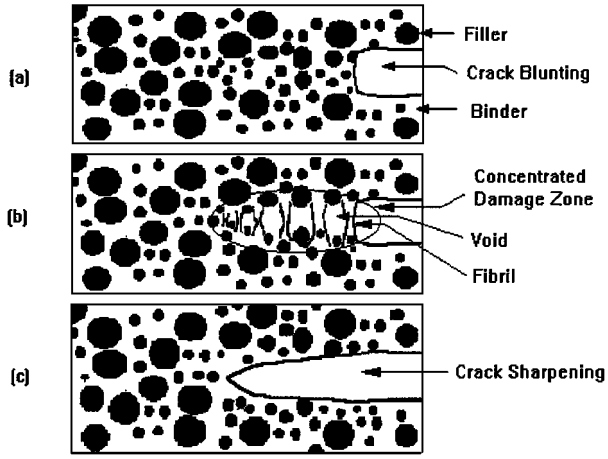

Figure 14 Model of crack propagation mechanism in propellant.

the rate at which bonds, for a constant stress, are ruptured increases resulting in higher crack velocities.

4. Conclusion

Image analysis and scanning electron microscopy has provided an understanding of the mechanism of crack propagation in composite propellants. The crack propagation mechanism in the composite propellant studied here can be described as one of blunt-growth-blunt [2]. This is summarised by Fig. 14a–c. A zone of dewetting ahead of the crack tip forms with increasing strain (Fig. 14b). Fibrils of dewetted HTPB binder and small voids surrounding the filler particles form and increase in size. The microvoids coalesce and the fibrils fail leading to crack resharpening (represented schematically in Fig. 14c). A new zone of damage then forms in the area ahead of the crack tip as the strain increases.

The fracture behaviour of the propellant specimens were affected by changes in temperature whilst strain-rate had only a marginal effect over the range studied. It was found that as the material temperature decreased from 60 to $-40\,^{\circ}$C the stiffening of the propellant caused a significant increase in the size of the damage zone and much higher levels of crack blunting resulted. The decrease in temperature was also accompanied by an increase in hysteresis ratio associated with higher levels of energy losses and decreased crack velocities. As the strain-rate increased the size of the damage zone, hysteresis ratio and crack velocity increased while the critical strain decreased.

A distinct correlation was found to exist between the severity of the thermal load to which the specimen had been subjected and the size of the damage zone, hysteresis ratio and crack velocity. The most significant change in the mechanism of crack growth was found in the propellant which had been subjected to accelerated ageing. A damage zone was not detected from image analysis of cracks propagating in accelerated aged specimens. The crack remained sharp at all times and propagated across the length of the specimens rapidly, the accelerated ageing had produced a change in the material that resulted in a more brittle type of fracture. By comparison no difference in the mechanism of crack growth was detected in the thermally shocked and thermally cycled specimens and the damage zones were similar in magnitude to those in the unaged specimens.

Acknowledgements

We gratefully acknowledge the assistance of Mr Brian Hamshere, Mr Alan Starks and Mr John Symes of WSD for supplying the propellant material used in this study and Mr Don Ashton and Mr Henry Gare for machining the specimens for testing.

References

1. C. LIU, in Fracture Mechanics: Twenty-Third Symposium, Philadelphia, 1993, edited by R. Chona (ASTM STP 1189, 1993) p. 668.
2. C. SMITH and C. LIU, in JANNAF Propulsion Meeting, Vol. 2, Nov. 1993, p. 1.
3. C. LIU, *Materials Evaluation* **47** (1989) 746.
4. C. LIU, AIAA Paper 93-1521-CP., 1993, p. 1837.
5. S.-Y. HO and C. FONG, *J. Mater. Sci*. **22** (1987) 3023.
6. C. SMITH, H. MOUILLE and C. LIU, in Advances in Experimental Mechanics and Biometrics, Anaheim, November 1992, edited by W. Jones and J. Whitney (ASME AMD-V146, 1992) p. 29.
7. S.-Y. HO, in Proceedings of the 16th TTCP WTP4 Conference, USA, 1991.
8. K. KISHORE, V. PAI VERNERKER and G. PRASAD, *Combustion and Flame* **36** (1979) 79.
9. KINLOCH and R. YOUNG, in "Fracture Behaviour of Polymers" (Elsevier Applied Science, Essex, 1985) p. 93.

Received and accepted 23 July 1998